Meijer *et al.*, *Nucleic Acids Res.* **18**, 7357 (1990).
4. R. Zwart, thesis, Erasmus University, Rotterdam (1996).
5. S. S. Scherer *et al.*, *J. Neurosci.* **14**, 1930 (1994).
6. E. S. Monuki, R. Kuhn, G. Lemke, *Mech. Dev.* **42**, 15 (1993); D. E. Weinstein, P. G. Burrola, G. Lemke, *Mol. Cell. Neurosci.* **6**, 212 (1995); X. He *et al.*, *Mol. Cell. Biol.* **11**, 1739 (1991).
7. P. Mountford *et al.*, *Proc. Natl. Acad. Sci. U.S.A.* **91**, 4303 (1994). Oct-6 genomic clones were isolated from a 129–genomic phage library and mapped with the use of several restriction enzymes. The targeting vector was linearized at the single Sal I site and electroporated into E14 ES cells maintained in BRL cell conditioned medium in the presence of Leukemia Inhibitory Factor. After selection in G418, correct replacement events were identified by Southern blot hybridization with the use of an internal 3′ probe and an external 5′ probe. Homologous recombination events had occurred in 15 of 51 G418-resistant ES cell lines. A number of these lines were karyotyped, and two cell lines with the correct number of chromosomes were injected in C57BL/6 blastocyst embryos. Both lines resulted in germline transmission. Heterozygous offspring were crossed to C57BL/6 mice and backcrossed at the F_2 generation.
8. R. Zwart, L. Broos, G. Grosveld, D. Meijer, *Mech. Dev.* **54**, 185 (1996).
9. Sciatic nerves were isolated from mutant mice and heterozygote littermates. One nerve was used for protein immunoblotting and another was used to isolate RNA. Nerves for protein immunoblotting were homogenized in sample buffer and loaded on a 15% (for P_0 and MBP) or 8% [for CNP and neurofilament medium chain (NF-M)] SDS-polyacrylamide gel. The gels were electroblotted on filters and further processed according to standard procedures. P_0 monoclonal antibody P07 was provided by J. J. Archelos [J. J. Archelos *et al.*, *J. Neurosci. Res.* **35**, 46 (1993)]. Other monoclonal antibodies were obtained from Boehringer Mannheim (MBP), Sigma (CNP), and Amersham (NF160). For RT-PCR, RNA was extracted with the LiCl-urea method and reverse-transcribed into cDNA with oligo(dT) and hexamer primers. Excess primers were removed on a Centricon C-30 (Amicon) concentrator. For MBP amplification, we used cDNA generated from P8 sciatic nerve RNA. After 20-fold dilution, polymerase chain reaction (PCR) amplification was performed by use of the Expand long template PCR system (Boehringer Mannheim). Each amplification cycle comprised 30 s at 94°C, 1 min at 55°C, and 1 min at 68°C. After the 10th amplification cycle, the extension time was increased with 20-s increments. Samples were taken at cycles 20, 22, 24, and 26. The following primers were used: MAG: 5′-primer GCCACGGTCATCTATGAGAGTCAGC and 3′-primer GGTGCCCAGAGATTCTGAATTCGG; HPRT: 5′-primer CACAGGACTAGAACACCTGC and 3′-primer GCTGGTGAAAAGGACCTCT; PMP-22: 5′-primer ACACTGCTACTCCTCATCAGTGAG and 3′-primer CAGGATCACATAGATGATACCACTG; and MBP: 5′-primer ACTCACACACGAGAACTACCCA and 3′-primer CCAGCTAAATCTGCTGAGGG. The amplified fragments yielded bands of 605 bp for MAG, 316 bp for PMP-22, 249 bp for HPRT, and 170 bp for MBP. Amplification products were separated on a 4% denaturing polyacrylamide gel, and signals were measured with a Molecular Dynamics phosphoimager.
10. Animals were perfused with phosphate-buffered saline, pH 7.2, for 3 min followed by fixative (3% paraformaldehyde and 1% glutaraldehyde buffered by 100 mM cacodylate at pH 7.2) for 10 min. Nerves were dissected, cut into smaller pieces, and fixed overnight in the same fixative. After postfixation in 1% osmium tetroxide, the sample was embedded in Epon. Ultra-thin sections were stained with uranyl acetate and lead citrate. Sections were examined and photographed with a Philips CM100 electron microscope.
11. R. Mirsky and K. R. Jessen, *Curr. Opin. Neurobiol.* **6**, 89 (1996).
12. We are grateful to D. Bootsma for his support, to E. Dzierzak for critical comments on the manuscript, and to M. Kuit, T. de Vries Lentsch, R. Koppenol, and R. Willemse for photography. We gratefully acknowledge J. Archelos for P_0 antibodies and L. Braam for animal care. All animal experiments were carried out under license 132-95-03 (Institutional Animal Care and Use Committee, Erasmus University).

1 March 1996; accepted 5 June 1996

Spinal Cord Repair in Adult Paraplegic Rats: Partial Restoration of Hind Limb Function

Henrich Cheng,* Yihai Cao, Lars Olson

Complete spinal cord gaps in adult rats were bridged with multiple intercostal nerve grafts that redirected specific pathways from white to gray matter. The grafted area was stabilized with fibrin glue containing acidic fibroblast growth factor and by compressive wiring of posterior spinal processes. Hind limb function improved progressively during the first 6 months, as assessed by two scoring systems. The corticospinal tract regenerated through the grafted area to the lumbar enlargement, as did several bulbospinal pathways. These data suggest a possible repair strategy for spinal cord injury.

Treatment that promotes functional regeneration across a complete spinal cord transection in humans does not exist. In animal experiments (*1*), recovery after incomplete spinal cord lesions has been achieved in mature animals treated with myelin-associated protein antibodies, whereas recovery after complete lesions has been shown in neonates (*2*). To avoid ambiguity and to model the most severe clinical scenario, we studied adult rats with complete surgical transection of the spinal cord, including removal of 5 mm of the cord at vertebra T8. Histology of excised pieces of spinal cord demonstrated complete transection (Fig. 1A). We then proceeded with a repair strategy (*3*).

We used peripheral nerve implants (*4*) to bridge the gap in the spinal cord (Fig. 1, B and C, and Fig. 2B) and found that the use of multiple fine nerve implants (18 nerves to bridge one gap) gave better precision than the use of fewer thicker nerves. To evade oligodendroglial proteins that inhibit axon regeneration (*5*), we rerouted regenerating pathways from nonpermissive white to permissive gray matter (*6*). The peripheral nerve bridges thus redirected descending motor pathways from proximal white to distal gray matter and ascending pathways from distal white to proximal gray matter (Fig. 1E), according to the specific anatomy of rat descending and ascending pathways (*7*). To stabilize the lesioned area and the peripheral nerve bridges, we filled the grafted area with a fibrin-based tissue glue that does not impair nerve fiber growth (*8*) and fixed the vertebral column in dorsiflexion by wiring (*9*).

Acidic fibroblast growth factor (aFGF) is a normal spinal cord constituent (*10*). Because it lacks a signal sequence, aFGF is thought to be sequestered within cells and released only after damage. Consequently, FGF may be involved in repair (*11*). It also decreases gliosis and enhances nerve fiber development in spinal cord grafts (*12*). Mixing aFGF into fibrin glue allows slow release of the factor (*13*).

Animals were followed over time for signs of functional recovery and rated by two independent, blinded observers using the combined behavioral score (CBS) (*14*) and the open-field walking score (OFWS) (*15*). Key responses were videotaped. Hind limb function in animals subjected to the repair procedure improved significantly, beginning 3 weeks after operation and continuing through the 1 year of observation (Fig. 1D). Animals subjected to unilateral treatment also improved, although to a lesser degree. Animals in four different control groups [transection only (n = 14), cord removal only (n = 5), white matter–to–white matter bridging (n = 3), and omission of aFGF (n = 2)] did not improve (Fig. 1D). Improvement was manifest as appearance of a functional posture in hind limbs (usually flexion at hips and then knees and then dorsiflexion at ankles). In controls, hind limbs remained extended and externally rotated. Improvement was symmetrical in six cases (28%) and asymmetrical in the rest. Locomotion involved four-limbed stepping (Fig. 2, H through J). Hind limbs

H. Cheng, Department of Neuroscience, Karolinska Institute, S-171 77 Stockholm, Sweden, and Department of Neurosurgery, Neurologic Institute, Veterans General Hospital-Taipei and Division of Surgery, National Yang-Ming University, Taiwan.
Y. Cao, Department of Cell and Molecular Biology, Karolinska Institute, S-171 77 Stockholm, Sweden.
L. Olson, Department of Neuroscience, Karolinska Institute, S-171 77 Stockholm, Sweden.

*To whom correspondence should be addressed. E-mail: henrich.cheng@neuro.ki.se.

partially supported body weight, and movements were noted in the three major joints. Such movements were not seen in any of the control groups. We also found statistically positive effects on contact placing scores of both groups with full treatment (Fig. 1D), which suggests that functional recovery involves the corticospinal tract (*2*).

Anterograde wheat germ agglutinin horseradish peroxidase (WGA-HRP) tracing from the sensorimotor cortices and retrograde WGA-HRP tracing from the lumbar enlargements were used to document fiber tract regeneration (Table 1) (*16*). The spinal cord and brain were analyzed, and labeled nerve cell bodies were counted (*17*). Sections from the engrafted area were analyzed with cresyl violet or antibodies against neurofilament and glial fibrillary acidic protein (GFAP) to illustrate morphology, nerve fibers in the bridges, and the degree of gliosis. Anterograde tracing is exemplified by one treated animal (Table 1 and Fig. 2, E through G) in which labeled fibers are shown descending in the dorsal funiculus of the proximal stump, traversing the bridging grafts, and reaching gray matter of the proximal portion of the distal stump. Fibers descended at the interface between the dorsal funiculus and dorsal gray matter and ended along the dorsomedial aspect of the dorsal horn in regions adjacent to substantia gelatinosa in the lumbar enlargement. The labeled fibers were thus found in areas corresponding to the pathway of the rat corticospinal tract, as shown in rodent cortical ablation studies (*7*). In the four other animals analyzed with anterograde tracing (Table 1), labeled fibers traversed the bridging grafts and were found in gray matter to T11, T11 through T12,

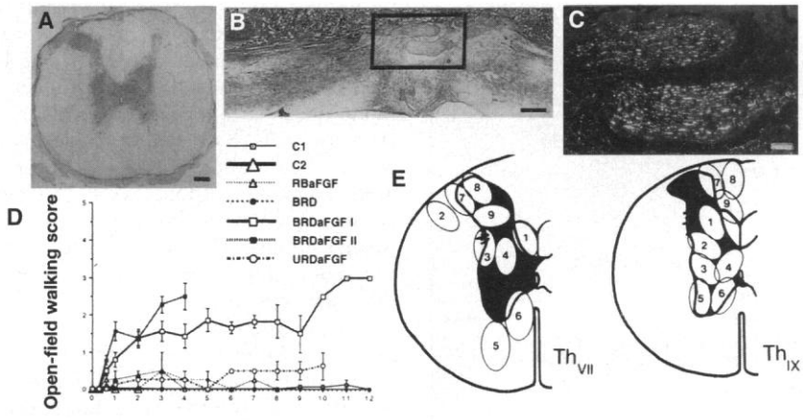

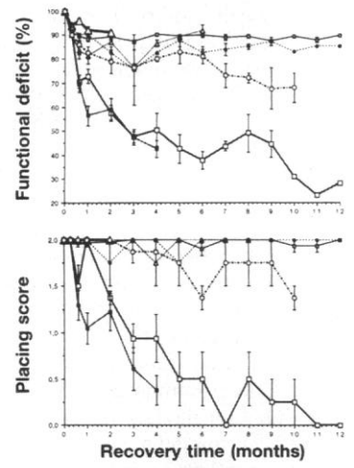

n for each group	Month	0	1	2	3	4	5	6	7	8	9	10	11	12
	C1	14	12	10	5	5	5	5	5	5	4	4	4	4
	C2	5	5	5	0	0	0	0	0	0	0	0	0	0
	RBaFGF	3	2	2	2	2	2	2	1	1	0	0	0	0
	BRD	2	2	2	2	2	2	2	2	2	2	2	2	2
	BRDaFGF I	5	5	5	4	4	4	4	3	3	2	2	1	1
	BRDaFGF II	17	15	10	8	4	0	0	0	0	0	0	0	0
	URDaFGF	2	2	2	2	2	2	2	2	2	2	2	0	0

Fig. 1. (**A**) Microphotograph illustrating a cresyl violet–stained transverse section through a removed spinal cord segment. Bar represents 250 μm. (**B**) Sagittal section of a repaired junction area stained with cresyl violet. Note the nerve bridge grafts. Boxed area indicates the redirected fasciculus gracilis (upper) and dorsal corticospinal tract (lower) between the proximal (left) and distal stumps (right). Bar represents 1000 μm. (**C**) Adjacent section immunostained with monoclonal antibody to neurofilament protein 70,000. Numerous nerve fibers are present in the intercostal nerve bridges. Bar represents 200 μm. (**D**) Hind limb function in the seven different groups (*3*). Hind limbs were assessed independently (except for the inclined plane test) to identify asymmetric recovery. Animal scores were generated by averaging hind limb scores. In the upper panel is shown the open-field walking score (*15*). Scores improved significantly more in the treated groups (BRDaFGF I and II) than in the controls (C1 and C2) from the third week on ($P < 0.0001$ for first 2 months; $P < 0.001$ for months 3 and 4; $P < 0.005$ for months 5 and 6; Mann-Whitney). Unilaterally treated animals (URDaFGF) improved to a lesser degree, as seen 6 months after surgery. In the middle panel is shown the percentage functional deficit, as indicated by the CBS. Animals subjected to the repair procedure improved significantly compared with both animals in which the spinal cord was only transected (C1) and animals in which a cord segment was removed (C2) ($P < 0.0001$ months 1 through 6; analysis of variance). In the lower panel is shown the contact placing score, which indicates functional recovery of the corticospinal tract and was significantly better in animals subjected to the repair procedure than in controls until 6 months ($P < 0.001$ for first 3 weeks; $P < 0.01$ for month 1; $P < 0.001$ for months 2 and 3; $P < 0.01$ for month 4; $P < 0.05$ for months 5 and 6; Mann-Whitney). (**E**) White matter–to–gray matter nerve bridges. Pieces of intercostal nerves were used to reconnect and redirect pathways between the spinal cord stumps (Th$_{VII}$ and Th$_{IX}$, seventh and ninth thoracic segments, respectively). For each redirected tract, one to three intercostal nerves were used. Bridge numbers and their intended functions are as follows: 1, dorsal corticospinal tract (crossed fibers); 2, rubrospinal tract; 3, central gray matter and formatio reticularis; 4, central gray matter and formatio reticularis; 5, ventral corticospinal tract (uncrossed fibers) and other tracts such as the vestibulospinal tract (VST) and the reticulospinal tract (RST); 6, ventral corticospinal tract (uncrossed fibers) and other tracts (VST and RST); 7, fasciculus gracilis; 8, fasciculus gracilis; 9, fasciculus gracilis; 10 to 18, as for 1 to 9 but on the other side.

Table 1. Summary of data from animals in which both open-field walking scoring (*15*) and HRP tracing data were collected. When tracing results were ranked from 0 (negative) to 10 (normal), the treated animals differed significantly from the controls ($P < 0.001$, Mann-Whitney). R, retrograde; A, anterograde.

Rat	Planned survival time (months)	Open-field walking score at death	HRP tracing result	
			R*	A†
		Full repair strategy		
1	12	3	817/1412	
2	9	1	0/840	
3	3	3	4048/2533	
4	3	2.5		+++
5	3	2		+
6	1	2.5		(+)
7	3	3		+
8	3	3		+
		Full repair except aFGF		
9	12	0	0/56	
		Repair with white-to-white bridges		
10	6	0		–
11	9	0	0/2	
		Spinal cord transection at T8 (no cord tissue removal)		
12	12	0	0/0	
13	12	0	0/8	
14	12	0	0/0	
15	2	0		–
16	2	0		–
17	2	0		–
18	3	0		–
		Normal		
19		5	21937/	‡
20		5	21871	
		Acute spinal cord transection		
21		0	0/0	
22		0		–
		Spinal cord colchicin injection at T8		
23		0	0/0	

*Cells in motor cortex/cells in brain stem. †(+), labeled tracts and cells seen in the bridges until T11; +, until T12 to L2; and +++, until L5 to S1. ‡Normal.

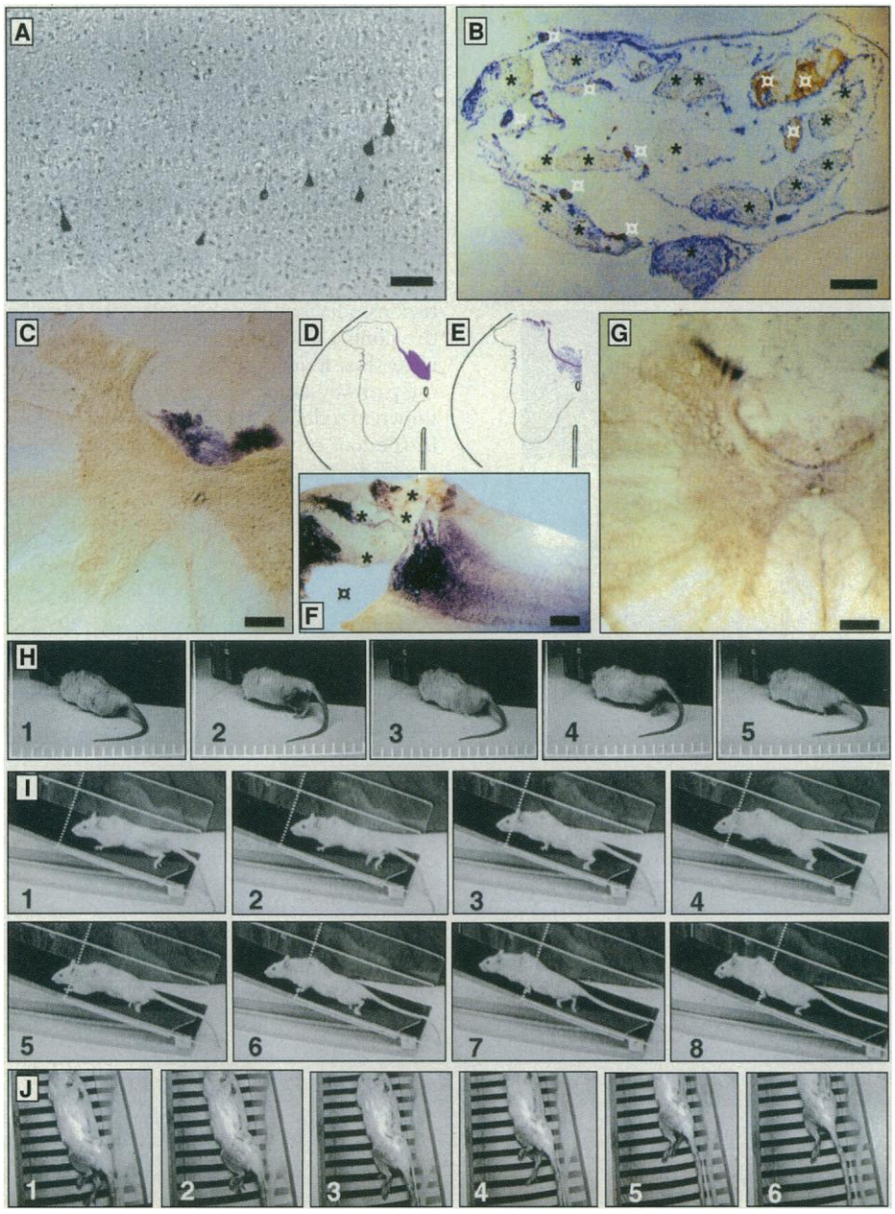

Fig. 2. Morphology and sequential videoframes of experimental animals. (**A**) Tetramethylbenzidine histochemistry of cortex cerebri (1 mm posterior to the bregma) in a rat 1 year after the repair procedure and 48 hours after retrograde WGA-HRP tracing from the lumbar enlargement. Labeled pyramidal cells are found in the hind limb motor area. Bar represents 100 μm. (**B**) Cresyl violet cross section of bridge area in a treated rat after 4 months. Note 15 nerve bundles (*) and blood vessels (¤). Bar represents 600 μm. (**C** through **G**) Anterograde transport of WGA-HRP after injection into the sensorimotor cortex in a normal rat [shown in (C) and schematically depicted in (D)] and in a treated rat 3 months after surgery [shown in (F) and (G) and schematically depicted in (E)]. In (F) the sagittal section of the bridge area shows labeled fibers traversing bridging grafts (*) and reaching the distal stump (right). The most proximal end of the distal stump was sectioned at an angle to the sagittal plane, allowing a face-on view of much of the regenerated bundle formed at the gray-white interface. Many fibers end in the proximal part of the distal stump, leading to dense labeling. A portion of the fibers reach the lumbar level depicted in (G). Some tissue was lost during free-floating processing of the section (¤). In (G) a transverse section of the lumbar enlargement shows labeled fibers in the dorsal funiculus at the white-gray interface, and adjacent to the substantia gelatinosa. Bars represent 200 μm in (C) and (G) and 500 μm in (F). (**H** through **J**) Sequential videoframes (interval between each frame was 0.12 s) of three rats subjected to the repair procedure. In (H) is shown an animal after 3 months. Hind limbs can support body weight during forward stepping. Toe dragging was absent in this animal. In (I) and (J) are shown rats climbing a 45° inclined plane 1 year (I) or 3 months (J) after surgery. Hind limbs partially supported body weight and displayed movements in all three major joints.

T12, or L1 through L2. In four transected control animals and in one animal subjected to white matter–to–white matter bridging plus aFGF, the corticospinal tracts did not reach the distal spinal cord stumps. Anterograde tracing of controls indicated no connections to the distal stumps (Table 1).

Application of WGA-HRP to the lesioned lumbar spinal cord led to labeling of motoneurons in layers III through V of hind limb motor areas bilaterally in cortex cerebri in two of the three treated animals (Fig. 2A). Labeled neurons were also observed in dorsal tegmentum and in the lower limb areas of the red nuclei, reticular nuclei, and raphe nuclei in all treated animals. A few raphe neurons (8 cells) were labeled in one of the three transected controls and in one animal grafted without aFGF (56 cells). Numerous raphe neurons were labeled in treated animals. Thus, a substantial number of regenerating descending axons, including the corticospinal tract and other supraspinal neurons, appear essential for functional recovery. Animals with improvement of hind limb function showed evidence of regeneration of both the motor initiation and the voluntary gait modification circuits to the spinal cord central pattern generator (*18*). The degree of functional recovery showed some correlation ($r = 0.86$) to the degree of regeneration of motor fiber systems (Table 1). GFAP immunohistochemistry showed large cysts and wide GFAP-poor gaps between the cord stumps (4.7 ± 0.86 mm, $n = 5$) in controls receiving transection only, whereas animals receiving the full repair strategy had significantly shorter GFAP-poor gaps (0.7 ± 0.19 mm, $n = 4$; $P < 0.001$, analysis of variance). The bridge grafts in the latter group displayed rich neurofilament immunoreactivity.

Many different models of spinal cord injury have been studied in animals. Incomplete spinal cord lesions such as hemisections, contusions, compressions, and different chemical or mechanical partial lesions have generated valuable information about reactive and compensatory changes, but several of these models are less suitable for studies of functional recovery caused by regeneration of cut axons. Our procedure can lead to a certain degree of structural and functional recovery in the completely transected adult rat spinal cord, including regeneration of pyramidal tract axons, hind limb movements, and weight support. It remains to be seen to what extent our technique is applicable to the chronic paraplegic state and to humans.

REFERENCES AND NOTES

1. E. Puchala and W. Windle, *Exp. Neurol.* **55**, 1 (1977); L. Olson *et al.*, *Brain Res. Bull.* **9**, 519 (1982).
2. Y. Iwashita, S. Kawaguchi, M. Murata, *Nature* **367**,

167 (1994); L. Schnell *et al.*, *ibid.*, p. 170; B. Bregman *et al.*, *ibid.* **378**, 498 (1995).
3. Vertebrae T7 through T10 were exposed in adult 250-g female Sprague-Dawley rats while the rats were anesthetized with halothane (1.5%; respiratory rate, ≈60 per minute; rectal temperature, <3°C below normal). After T8 and T9 posterior laminectomies and bipolar cauterization to control hemorrhage, a 5-mm T8 spinal cord segment was removed with microscissors (Fig. 1A). Eighteen intercostal nerves collected in Hanks' buffered saline solution (HBSS) were used to reconnect and redirect pathways between the spinal cord stumps (Fig. 1E). The floor of the cavity between the spinal cord stumps was covered by a thin gelfoam layer. Minced pieces of peripheral nerve were used to fill the angle between the gelfoam bottom and the ventralmost (white matter) surface of the cut end of the distal spinal cord stump, producing a slanted floor that allowed some physical support of the nerve bridges that went from deep (white matter) proximal sites to somewhat more dorsal (gray matter) distal sites. The cut ends of the intercostal nerve bridges were attached to the semidry spinal cord stump surfaces. The two fibrin glue sealant elements (Beriplast P, generously provided by Behring, Germany) were prepared (*8, 13*). The final glue solution, of which 10 μl was applied to the engrafted area, consisted of aFGF (2.1 μg/ml), fibrinogen (100 mg/ml), aprotinin (200 kIU/ml), thrombin (40 IU/ml), and 8 mM $CaCl_2$. The T7 and T10 spinal processes were fixed in dorsiflexion with an S-shaped monofilament surgical steel (DS-20, Ethicon) loop and fastened to the spinal column with nonabsorbable circumspinal threads. One experimental group was subjected to unilateral redirection, and aFGF was included in the glue (URDaFGF); the other two groups were subjected to bilateral redirection and aFGF glue through use of autografts (50%) mixed with allografts (BRDaFGF I) or through use of only autografts (BRDaFGF II). Control animals were subjected to transection at T8 (C1), to removal of a 5-mm cord segment (C2), or to grafting with the same methods as in the experimental groups except that HBSS replaced aFGF (BRD) or that grafting was done with only white matter–to–white matter connections (RBaFGF). Animals were caged on thick soft bedding, with heating from below during the first postoperative days. The rats' bladders were emptied manually twice daily as long as needed. Antibiotics (Borgal, Hoechst, 15 mg per kilogram of body weight, subcutaneously) were injected once daily for 7 days. Decubitus sores on hind limbs were treated with iodine-soaked dressings. Animals were killed if severe sepsis (urinary tract infection), infected decubitus sores, or other wounds occurred. For the major experiments described here, mortality was <10%. Experiments were approved by the animal research ethical committee of Stockholm. Animals were killed at different time points for histological analyses but no earlier than 1 month after surgery to ensure complete degeneration of the cut descending fibers in the distal stump (*9*).
4. S. David and A. Aguayo, *Science* **214**, 931 (1981); M. Benfey and A. Aguayo, *Nature* **296**, 150 (1982); R. Bunge, *Curr. Opin. Neurobiol.* **3**, 805 (1993).
5. T. Savio and M. Schwab, *Proc. Natl. Acad. Sci. U.S.A.* **87**, 4130 (1990); M. Schwab, *Trends Neurosci.* **13**, 452 (1990).
6. L. Nygren, K. Fuxe, G. Jonsson, L. Olson, *Brain Res.* **78**, 377 (1974); R. Kuang, M. Merline, K. Kalil, *Development* **120**, 1937 (1994).
7. L. Brown, *Exp. Brain Res.* **13**, 432 (1971).
8. H. Cheng, S. Almström, L. Olson, *J. Neural Transplant. Plast.* **5**, 233 (1995).
9. H. Cheng and L. Olson, *Exp. Neurol.* **136**, 149 (1995).
10. R. Elde *et al.*, *Neuron* **7**, 349 (1991); Y. Cao, thesis, Karolinska Institute (1993); M. Koshinaga, H. Sanon, S. Whittemore, *Exp. Neurol.* **120**, 32 (1993).
11. P. McNeil, L. Muthukrishnan, E. Warder, P. D'Amore, *J. Cell Biol.* **109**, 811 (1989).
12. M. Giacobini, B. Hoffer, G. Zerbe, L. Olson, *Exp. Brain Res.* **86**, 73 (1991).
13. H. Cheng *et al.*, *ibid.* **104**, 199 (1995).
14. K. Gale, H. Kerasidis, J. Wrathall, *Exp. Neurol.* **88**, 123 (1985). Percentage functional deficit as indicated by the CBS was used for behavioral evaluation. The CBS (except hot plate), which ranges from 100 points (complete paralysis) to 0 (normal), comprises scores of motor skills (0 to 45), toe spread (0 to 5), righting reflex (0 to 15), extension withdrawal (0 to 5), placing reflex (0 to 5), climbing on an inclined plane (0 to 15), and swimming (0 to 10).
15. M. Beattie and J. Bresnahan, in *Criteria for the Assessment of Recovery of Function: Behavioral Methods*, M. Brown *et al.*, Eds. (American Paralysis Association, Springfield, NJ, 1989), pp. 16–25; D. Behrmann, J. Bresnahan, M. Beattie, B. Shah, *J. Neurotrauma* **9**, 197 (1992). Open-field walking measured the animal's gross locomotor ability during a 5-min testing period. Two coded animals were observed simultaneously to stimulate locomotor activity and were scored according to a modified Tarlov scale, which ranged from 0 (flaccid paralysis) to 5 (normal walking). This scale was subdivided to more accurately reflect the pattern of recovery of locomotor function as follows: 0, no spontaneous movement; 1, movement that was not reflexive and movement in the hip or knee but not ankle; 2, movement of the limb in all three major joints; 3, active support and an uncoordinated gait or occasional short bouts of coordinated gait; 4, coordination of forelimbs and hind limbs in gait (trotting), including some walking on knuckles or the medial surface of the foot or a few toe drags; and 5, normal.
16. L. Heimer, in *Neuroanatomical Tract-Tracing Methods*, L. Heimer, M. Robards, L. Zaborszky, Eds. (Plenum, New York, 1989). For retrograde HRP tracing, six 0.1-μl injections of 5% WGA-HRP (Sigma) were made into the lumbar enlargement (L4 to L5, 25 mm distal to the distal graft-host interface) and combined with an L6 transection to enhance HRP uptake. Positive and negative controls included injection of WGA-HRP with and without colchicin blockage or an acute cut at T8 (Table 1). For anterograde HRP tracing, a total of 2 μl of 5% WGA-HRP was injected into the sensorimotor cortices as five 0.2-μl injections per side. Positive and negative controls are also given in Table 1. Animals were perfused 48 hours later (Ringer's solution, 2% paraformaldehyde, and 10% sucrose). For immunohistochemistry of grafted areas, tissues were further treated with 4% paraformaldehyde for 2 hours and then with polyvinylpyrrolidone (Sigma) for 6 weeks to allow sectioning of soft and bony tissue together. Cryostat 14-μm sections for immunohistochemistry and 60- (brain and brainstem) or 90-μm (spinal cord) free-floating sections for tetramethylbenzidine histochemistry were collected.
17. M. Abercrombie, *Anat. Rec.* **94**, 239 (1946). HRP-labeled neuron counts required the presence of the nucleus. The total number of neurons (N) equals $nt/(t + d)$, where n is the number of nuclei of HRP-labeled neurons counted times the section period, t is the section thickness, and d is the average diameter of counted nuclei.
18. S. Grillner, in *Control of Posture and Locomotion*, R. Stein, K. Person, R. Smith, J. Redford, Eds. (Plenum, New York, 1973), pp. 515–535.
19. We dedicate this paper to Arne Nylander. Supported by the American Paralysis Association, the Swedish Medical Research Council, USPHS grants, the Taiwan Chin-Lin Fund, and the National Science Council. We thank the late J. Arvidsson for advice and S. Almström, M. Casserlöv, K. Erlandsson, and I. Engqvist for assistance. aFGF was provided by Y. Cao and R. Pettersson, Ludwig Institute for Cancer Research, Stockholm.

2 November 1995; accepted 31 May 1996

Persistent Site-Specific Remodeling of a Nucleosome Array by Transient Action of the SWI/SNF Complex

T. Owen-Hughes, R. T. Utley, J. Côté, C. L. Peterson, J. L. Workman*

The SWI/SNF complex participates in the restructuring of chromatin for transcription. The function of the yeast SWI/SNF complex in the remodeling of a nucleosome array has now been analyzed in vitro. Binding of the purified SWI/SNF complex to a nucleosome array disrupted multiple nucleosomes in an adenosine triphosphate–dependent reaction. However, removal of SWI/SNF left a deoxyribonuclease I–hypersensitive site specifically at a nucleosome that was bound by derivatives of the transcription factor Gal4p. Analysis of individual nucleosomes revealed that the SWI/SNF complex catalyzed eviction of histones from the Gal4-bound nucleosomes. Thus, the transient action of the SWI/SNF complex facilitated irreversible disruption of transcription factor–bound nucleosomes.

The remodeling of chromatin structures to generate deoxyribonuclease (DNase)-hypersensitive sites at regulatory elements precedes or occurs concurrently with the induction of transcription at many genes (*1*). Genetic and biochemical studies implicate an adenosine triphosphate (ATP)–dependent multisubunit protein complex, the SWI/SNF complex, in this process (*2*). The 2000-kD SWI/SNF complex binds to DNA and nucleosomes, perturbs histone-DNA interactions, and enhances the affinity of transcription factors for nucleosomal DNA (*3–7*). To investigate the mechanism by which SWI/SNF might remodel chromatin at transcriptional regulatory elements, we analyzed the action of the *Saccharomyces*

T. Owen-Hughes, R. T. Utley, J. Côté, J. L. Workman, Department of Biochemistry and Molecular Biology and Center for Gene Regulation, Pennsylvania State University, University Park, PA 16802–4500, USA.
C. L. Peterson, Program in Molecular Medicine and Department of Biochemistry and Molecular Biology, University of Massachusetts Medical Center, Worcester, MA 01605, USA.

*To whom correspondence should be addressed. E-mail: JLW10@psu.edu